CrystEngComm

Accepted Manuscript

ROYAL SOCIETY OF CHEMISTRY

www.rsc.org/crystengcomm

Journal Name

RSCPublishing

ARTICLE

Discovery of new crystalline phase, $BiGeO_2(OH)_2(NO_3)$

Cite this: DOI: 10.1039/x0xx00000x

Kiyoshi Kobayashi,*[a] Takuji Ikeda,[b] Norihito Hiyoshi,[b] and Yoshio Sakka[a]

Received 00th January 2012,
Accepted 00th January 2012

DOI: 10.1039/x0xx00000x

www.rsc.org/

A new crystalline phase has been discovered in the Bi_2O_3-GeO_2-HNO_3-H_2O quartet system. The new phase was slowly precipitated at room temperature under atmospheric pressure from a strongly acidic aqueous solution (pH ~0.2) containing dissolved bismuth oxide, germanium oxide, dilute ammonia, and nitric acid. Characterizations and crystal structure analyses were carried out by means of powder X-ray diffraction (PXRD), scanning electron microscopy (SEM), energy dispersive X-ray (EDX) spectroscopy, high-angle annular dark-field scanning transmission electron microscope (HAADF-STEM), thermogravimetry (TG)–mass spectrometric analysis, and solid-state nuclear magnetic resonance (NMR) spectroscopy. The molecular formula was established as $BiGeO_2(OH)_2(NO_3)$. The crystal structure of this new phase was elucidated by a combination of direct and charge-flipping methods from PXRD data. The new phase was found to have the space group *Pbca* with lattice parameters of a = 1.145510(10) nm, b = 0.495346(5) nm, and c = 1.81676(2) nm. This new phase was observed to possess a layered structure consisting of BiO_6 polyhedra, GeO_5 trigonal bipyramids and nitrate ions.

Introduction

Germanate crystals and glasses have attracted the attention of researchers for use in a wide range of applications such as γ-ray and X-ray scintillators,[1-6] X-ray phosphors,[7, 8] solid electrolytes,[9-12] and optoelectronics[13-15] among others because of its good optical and electrical properties and relatively easy to prepare the glasses and single crystals. Most of these materials are typically synthesized by conventional solid-state reactions and/or the sol–gel method using metal alkoxides and organic solvents owing to the poor solubility of most germanium salts in water, with the exception of alkali germanates.[7, 16-19] In the case of germanate oxide synthetic protocols involving the use of multiple metal components, alkali germanate solutions are difficult to employ in the preparation of homogeneous aqueous solutions containing both metal and germanium ions, as the species are dissolved under dissimilar conditions (acid and alkaline conditions, respectively). An inhomogeneous gelation has been previously applied toward the low-temperature synthesis of hafnium germanate.[7] In other methods, dilute GeO_2 aqueous solutions are necessary for preparation of the solution due to the very poor water solubility of GeO_2.[20-26] Hence, developing a facile preparative method for homogeneous aqueous germanate-containing solutions is of key importance in furthering synthetic technologies directed at the low-temperature synthesis of various germanate materials.

By chance, we had previously discovered a preparative method for the generation of homogeneous solutions containing ammonium germanate and other various metal salts during the development of low-temperature synthetic protocols toward various germanate oxides in aqueous solution.[27, 28] During these investigations, we discovered the formation of a previously unknown structural phase from an aqueous solution consisting of dissolved bismuth oxide, germanium dioxide, dilute ammonia, and nitric acid; the phase was observed to form under strongly acidic aqueous conditions (pH ~0.2) without the need for special treatment, e.g., hydrothermal conditions. In addition, we succeeded in solving the crystal structure of the unknown phase by a combination analysis of the direct and charge-flipping methods using data collected from the powder X-ray diffraction (PXRD) technique. In this paper, we report the preparation procedure, characterization, and crystal structure analysis of the new phase, a bismuth germanium oxyhydroxy nitrate.

Experimental

Preparation of the Solid Phase

The previously unknown solid phase was synthesized from a homogeneous aqueous solution. The raw materials employed were Bi_2O_3 (99.9% purity, Rare Metallic Co., Ltd., Japan), GeO_2 (99.99% purity, Rare Metallic Co., Ltd., Japan), nitric acid (ρ = ~1.38, Nacalai Tesque, Inc., Japan), ammonia solution (28% NH_3 aq., Wako Pure Chemical Co., Ltd., Japan), and distilled water. The commercial ammonia solution was diluted to 10 vol% NH_3 aq. with distilled water (hereinafter referred to

as "diluted ammonia"). Bi_2O_3 (1.87 g) was dissolved in nitric acid (11 mL) and distilled water (5 mL) in a beaker (referred to in the text as "Bi solution"). In another beaker, 0.63 g of GeO_2 was dispersed in 20 mL distilled water. The opaque GeO_2-dispersed water became transparent by addition of dilute ammonia in 20 portions of 100 μL each, for a total added volume of 2 mL. Period for each portions was about 10 s. During the addition of dilute ammonia, the opaque GeO_2-dispersed water was stirred using magnetic stirrer. This clear aqueous solution obtained was named "Ge solution." The solubility of GeO_2 in dilute ammonia has already been reported by several groups.[7, 16, 17] Both Ge and Bi solutions were slowly mixed together, resulting in a homogeneous solution. The temperature of the mixed solution rose to about 323 K as the result of heat generated by acid–alkali reactions taking place. At this stage, pH of the homogeneous solution appeared as less than 0, as the pH meter employed (MP120, Mettler Toledo, AG, Switzerland) displayed a value out of its measurement range. Next, the prepared ammonia solution was slowly added dropwise into the solution until reaching a pH of about 0.2. No precipitate or colloid formation was observed under these conditions.

The top of the beaker containing the prepared solution was sealed with Parafilm and the mixed aqueous solution was statically annealed at room temperature. After about five days of standing, a white powder was observed to begin precipitating. After the solution had been kept for one week, the precipitate was filtered off out. The filtered precipitate was washed using distilled water and filtered again. This washing and filtering procedure was repeated three times and the resulting precipitate was then dried at 373 K under air. This dried precipitate obtained is hereafter labelled as "BGNHO powder."

Sample Characterization

Identity confirmation of the formed phases for the prepared samples was carried out by a PXRD analysis using a diffractometer (RINT-2500, Rigaku Co., Ltd., Japan). For accurate structural analyses, high-resolution PXPD data were collected at room temperature on a SmartLab (Rigaku Co., Ltd., Japan) powder diffractometer with Bragg–Brentano geometry and Cu Kα radiation using a Ni filter. The diffractometer was equipped with a linear high-speed detector and operated at 40 kV and 50 mA. The flat specimen stage was spun at 60 rpm during measurement in order to reduce the preferred orientation effect as much as possible.

The presence of proton and nitrogen atoms could be assumed on the basis of raw materials used. The local environment of proton and nitrogen nuclei in the obtained solid was investigated by means of a solid-state magic-angle spinning nuclear magnetic resonance (MAS NMR) experiment. Solid state ^1H–^{15}N cross-polarization (CP) MAS NMR spectra were obtained at a spinning frequency of 5 kHz using a 4 mm MAS probe, a 90° pulse length of 3.5 μs, and a cycle delay time of 30 s on an AVANCEIII 400 WB spectrometer (Bruker BioSpin, Ltd., Japan) operated at 40.56 MHz. ^1H MAS NMR spectra were measured at a spinning frequency of 14 kHz and a single pulse sequence operated at 400.13 MHz. The ^1H and ^{15}N chemical shifts were referenced to distilled water and glycine (used as a secondary reference), respectively.

Thermal and evolved gas analyses were conducted by thermogravimetric–differential thermal analysis–mass spectroscopy (TG-DTA-MS, TG-DTA2100SR/MS9610, NETZSCH, Japan). The measurement temperature range was between room temperature and 1065 K under a He gas flow. The rate of temperature increase was set at 10 K/min.

Microscopic morphology of the obtained powder was observed by a field-emission scanning electron microscope (SEM; S-4800, Hitachi Co. Ltd., Japan) operated at an acceleration voltage of 2 kV. Energy dispersive X-ray (EDX) spectroscopy was carried using the XFlash silicon drift detector (Quantax 200, Bruker AXS, Ltd., Japan). Atomic resolution structural image was corrected by a C_s-corrected high-angle annular dark-field scanning transmission electron microscope (HAADF-STEM, JEM-ARM200F JEOL Co. Ltd., Japan) operated at an acceleration voltage of 200 kV and a convergence semi-angle of 13 mrad. The collection semi-angles for the HAADF imaging techniques were adjusted in the range 54–170 mrad.

Additionally, the local motions of guest molecules were investigated using Fourier-transformed infrared (FT-IR) spectroscopic measurements performed using an FT/IR-4100 spectrometer (JASCO Co., Japan). Transmission spectra were collected at room temperature in the range from 400–4000 cm^{-1} by the KBr method at a nominal resolution of 4 cm^{-1}, taking the spectrum of a KBr pellet as the background.

Results and Discussion

Features of the Homogeneous Solution

As confirmed experimentally, the complete dissolution of GeO_2 into water could not be observed due to the presence of a colloidal precipitation residue in the following cases: (I) an undiluted ammonia solution (28% NH_3) was added using the same procedures as detailed in the Experimental section; (II) A 2 mL volume of dilute ammonia was rapidly added in one portion into the GeO_2-dispersed water even though the Ge solution contained the same total amount of ammonia, and; (III) nitric acid was contaminant in the GeO_2-dispersed water. However, after the dissolution of GeO_2 by slow addition of dilute ammonia, rapid precipitation was not observed by addition of nitric acid to the Ge solution. Instead, a crystalline GeO_2 having a quartz-like structure was gradually precipitated on the walls of the beaker interior and/or on the quartz-glass-substrate surface when placed in an acidic Ge solution by addition of excess nitric acid. Several days were necessary for the gradual precipitation depending on the GeO_2 concentration and pH. In contrast, the Ge solution at pH = 9 was stable, with no precipitate formed under storage in a capped bottle. With respect to the Bi solution, anomalous features were not observed in terms of precipitation and dissolution by addition

of acid and alkaline reagents. More importantly, the order of steps in the procedure described in the Experimental section was crucial in terms of preparation of the mixed homogeneous solution containing Bi_2O_3, GeO_2, nitric acid, and ammonia; we could not obtain the phase by preparing the homogeneous solution by addition of the same volume of ammonia to a GeO_2 dispersion in the Bi solution, even though the proportions of reagents were identical.

After preparation of the homogeneous solution, rapid precipitate formation was not observed by simply mixing the Bi and Ge solutions without pH adjustment. However, precipitate formation was rapidly observed when the pH was adjusted to higher than 0.4 by ammonia addition. Moreover, the precipitate was reversibly dissolved by addition of nitric acid. Although no precipitate was immediately formed after mixing the Bi and Ge solutions and subsequent adjustment of pH to 0.2 using ammonia, slow precipitate formation was observed by annealing at room temperature for longer than several days. Furthermore, a period of over 20 days was necessary to obtain the precipitate when the mixture solution was diluted by one order of magnitude using distilled water. Therefore, the as-prepared solution appeared to be in an oversaturated state. Although we could not conclude whether the BGNHO phase is stable or metastable at this stage, the BGNHO phase did not decompose after precipitation when it was preserved in aqueous solution. In addition, we have confirmed that the BGNHO phase can be reproducibly obtained by the above procedures.

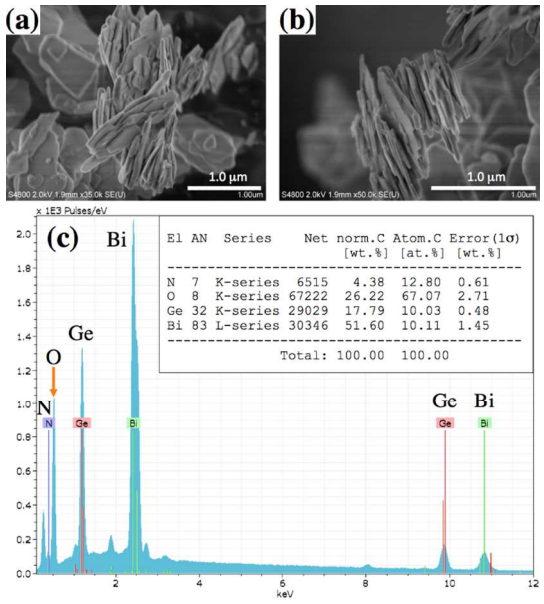

Fig. 1. Morphology of the BGNHO powder observed by (SEM). Plate shapes from the top and oblique views (a) and from the side view (b) are presented. The EDX spectrum showed the Bi:Ge ratio of nearly 1:1 (c).

Physicochemical Analysis of BGNHO Phase

SEM images of the BGNHO phase at various orientations are shown in Fig. 1(a) and (b). In addition, the SEM-EDX spectrum is presented at Fig. 1 (c). The phase morphology appeared to consist of thin plates with a length of ca. 0.2–0.8 μm and a thickness of ca. 20–60 nm, and extended stacking of the thin plate-like crystals could be observed. The surface of the particle was flat without adhesion of the contamination, suggesting that a single phase of BGNHO was obtained. SEM-EDX analysis indicated that the phase was obtained with a Bi:Ge ratio of nearly 1:1 (Fig. 1(c)).

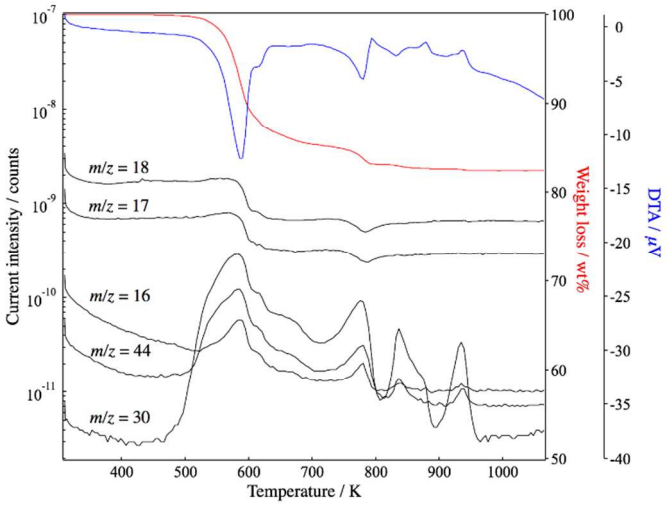

Fig. 2. TG-DTA-MS spectra of BGNHO measured under He gas flow. Temperature scan rate was 10 K / min.

From the TG-DTA-MS spectra of BGNHO, no weight loss was observed below 473 K, suggesting no adsorbed water in the sample (Fig. 2). A large weight loss of ca. 14.2 wt% with a sharp endothermic peak took place in the temperature range from 523–643 K. Furthermore, a smaller weight loss of ca. 1.5 wt% was also observed with an obvious endothermic peak at 763–823 K. These weight losses are probably due to release of water molecules by internal dehydration–condensation reactions and decomposition reaction from nitrate to oxide. Similar endothermic reaction accompanied with weight loss was reported for the bismuth basic nitrates. [29, 30] The gross weight loss was estimated as ca. 17.6 wt%.

From MS analysis, a large change in the specific fragment mass, that is, m/z = 16, 17, 18, 30, and 44, was observed with variations in temperature. The mass number m/z = 16 could be attributed to O_2 fragments; shortly after heating, the molecule began to be eliminated. The mass numbers m/z = 17 and 18 could be attributed to OH ion and H_2O molecule; their current intensity ratio was OH:H_2O = 1:5 and the decay of them was proportional to the TG profiles. Therefore, most of the observed H_2O could be attributed to atmospheric water, indicating the absence of isolated H_2O molecules in the BGNHO. The mass numbers m/z = 30 and 44 could be attributed to nitrosonium ion (NO) and dinitrogen monoxide (N_2O), respectively. These fragments are derived from decomposition of HNO_3. Therefore, we assumed that NO_3^- ion is included in BGNHO as the most probable chemical species; this result is supported by the ^1H–^{15}N CP/MAS NMR experiment as described below. The current intensities at m/z = 14, 28, 29 and 40 were monotonically

decreased with increasing temperature. These fragments could be attributed to N, N_2 and Ar in atmosphere mainly.

The FT-IR spectrum of BGNHO is shown in Fig. 3. The absorption bands around 1640 cm^{-1} and 3200 cm^{-1} likely corresponded to adsorbed H_2O, while the sharp band at 3460 cm^{-1} could be attributed to O-H hydroxyl ion.[31, 32] The absorption bands at 1350, 1385, and 1450 cm^{-1} could be attributed to a H–O–N bending vibration.[33] The absorption band at 1289 cm^{-1} was likely that of the nitrite ion, which indicates that the uptake of HNO_3 onto the BGNHO crystal is accompanied by a surface reaction that forms NO_2^-.[34] The broad bands around 1010 cm^{-1} could be assigned to the NO_3^- ions.[35] The absorption band at 659 cm^{-1}, 705 cm^{-1}, and 736 cm^{-1} might be assigned to the Ge–O stretching vibration.[32] The absorption peaks between 650 cm^{-1} and 810 cm^{-1} have a possibility of molecular bands in GeOH vibration.[32] The other absorption bands, which are not clarified at the present time, would likely be attributed to the bond motions of more heavy.

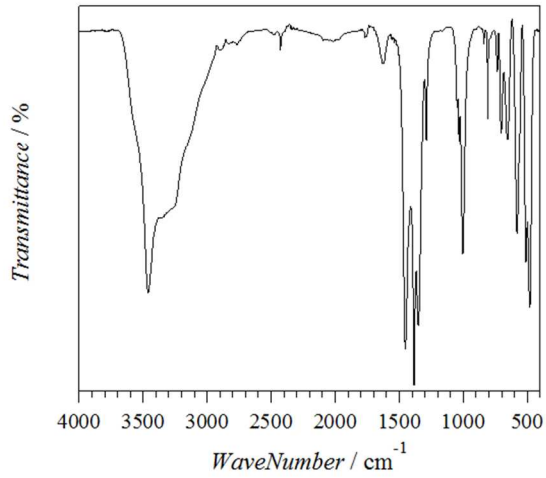

Fig. 3. FT-IR spectra of BGNHO.

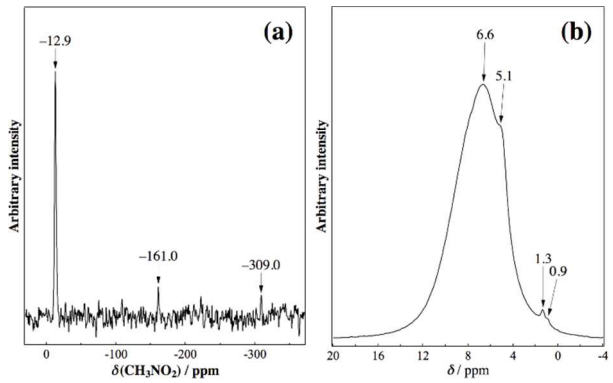

Fig. 4. (a) ^1H–^{15}N CP/MAS NMR and (b) ^1H MAS NMR spectra of BGNHO.

Solid-State NMR of BGNHO Phase.

The ^1H–^{15}N CP/MAS NMR and ^1H MAS NMR spectra of BGNHO are shown in Fig. 4(a) and (b), respectively. In ^{15}N NMR spectra (Fig. 4(a)), a sharp resonance peak observed at –12.9 ppm could be attributed to the formation of nitrate (M–ONO_2; M is metal) species.[36-38] This finding suggests that some of the included NO_3^- ions are coordinated to Bi (or Ge) atoms in BGNHO. Two small resonance peaks observed at –161 ppm and –309 ppm are attributed to interstitial nitride and residual ammine (M–NH_3), respectively.

The two broad resonance peaks at 5.1 and 6.6 ppm in the ^1H MAS NMR spectrum of BGNHO (Fig. 4(b)) could be attributed to various kinds of hydrogen-bonding motifs, e.g., –O···HO– formation between adjacent terminal OH groups bonding with Bi (or Ge) sites or $NO_3^-H^+\cdots$O–Bi (or Ge) formation between OH group and nitrate. The atomic distances of O–O were estimated as 0.284 nm for 6.6 ppm signal and 0.290 nm for 5.1 ppm signal, according to an empirical equation; δ/(ppm) = 79.05–255 × d/(nm).[39] Because of broad spectra width of a main peak, the proton distribution would be disorderly in a crystal structure and the O–O distance of the hydrogen bond may be inhomogeneous of approximately 0.27~0.29 nm. Two small resonance peaks observed at 0.9 ppm and 1.3 ppm means existence of a further long-distance hydrogen bond of > 0.3 nm.

Crystal Structure of BGNHO Phase

From a phase search using the ICDD PDF-2 database (release 2011),[40] the crystal structure of BGNHO could not be identified as a known crystal phase. Accordingly, the structure was determined by ab initio structural analysis using powder diffraction data. Indexing of reflections with the *N*-TREOR program with the built-in EXPO2013 program[41] successfully gave the lattice parameters and indices of reflections. The indexing of the reflections gave an orthorhombic unit cell of a = 1.145 nm, b = 0.4953 nm, and c = 1.817 nm with acceptable figures of merit (F20 = 39 and M20 = 25). The space group was determined from reflection conditions derived from these indices. Reflection conditions derived from the indexed reflections were k = 2n for 0kl, l = 2n for h0l, h = 2n for hk0, h = 2n for h00, k = 2n for 0k0, and l = 2n for 00l, which gives the space group *Pbca* with the highest symmetry. Observed integrated intensities, $|F_{obs}|^2$, were extracted by the Le Bail method[42] using EXPO2013. Then, a structural model for BGNHO was constructed by combination of the powder charge-flipping (pCF) method[43] using the program Superflip[44], and the direct method with EXPO2013.

At first, one Bi and one Ge site and four O sites were found by the combination analysis of direct method and pCF. It was found that a layered framework composed of BiO_n and GeO_4 was included in a unit cell. In addition to this, two Bi–Ge–O layers were found to be stacked along the [001] direction. Although it was confirmed that the GeO_4 chain lay along the b-axis, the positioning of oxygen atoms around Bi atom was not clarified at this stage. The GeO_4 tetrahedra were slightly deformed from regular tetrahedral shape, and the formation of GeO_5 trigonal bipyramid (tbp) structure (described later) was estimated.[45, 46] The coordination number of Bi is usually 3–8 with an atomic distance, l(Bi–O), of ca. 0.22–0.3 nm; this wide coordination number is attributed to the inert-pair effect of the Bi atom.[47] Next, distribution of NO_3^- ion in the interlayer was

investigated by the direct-space method with the program FOX.[48] In this analysis, the molecular structure of NO_3^- ion was introduced into a structural model as a rigid body fragment. The positions of all the framework atoms were fixed at the positions determined by the combination analysis as described above. It turned out that one oxygen atom of NO_3^- ion is located near the Bi atom, indicating NO_3^- ion acts as a ligand molecule of a Bi atom.

Lattice and structure parameters of BGNHO were refined using the program RIETAN-FP[49] on the basis of the initial model as described above. A split pseudo-Voigt profile function and a background function of Legendre polynomials with 11th order were used in the refinement. Partial profile relaxation with a modified split pseudo-Voigt function was applied to some reflections with anisotropic broadening profiles. In this refinement, taking a proton site into consideration was omitted for the convenient.

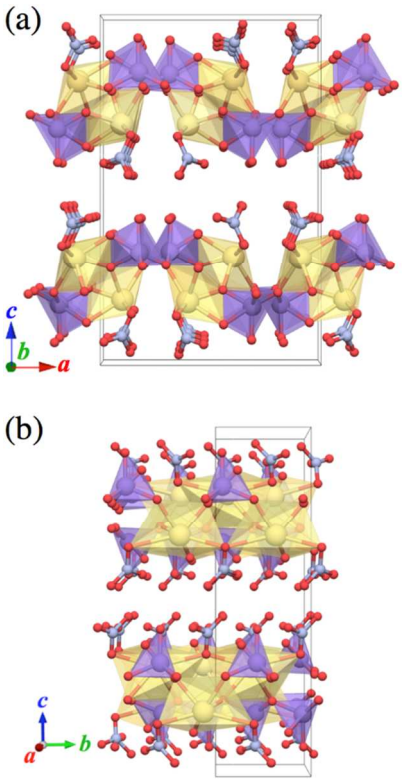

Fig. 5. Crystal structure model of BGNHO viewed along the [010] direction (a) and [100] direction (b), respectively.

The crystal structure model of BGNHO viewed along the [010] and [100] directions are illustrated at Fig. 5(a) and (b), respectively (see Table 2). It was found that the tbp structure of GeO_5 which share four O atoms with a Bi atom is formed. Most probable coordination number at Bi atom was six within the range of l(Bi–O) < 0.28 nm. An average interlayer distance was estimated as ca. 0.3 nm. NO_3^- ions are distributed in the interlayer and coordinate with Bi atom. The atomic distance of N–N between neighboring NO_3^- ions is ca. 0.41 nm. A chain of GeO_5 tbp lies along [010] direction. The irregular shaped BiO_6 polyhedra accompanied with two NO_3^- ions are distributed parallel to the GeO_5 tbp chain, and adjacent BiO_6 polyhedra shares sites O2, O4 and O7. The Bi–Ge–O arrangements were established as honeycomb-like layered structure composed of two kinds of six-membered ring. A local arrangement of GeO_5 tbp and BO_6 polyhedra is shown in Fig. 6. The shape of GeO_5 tbp is deformed from regular tbp shape and the angle of O1–Ge–O4 was approximately 174°. Actually, the shape of GeO_4 composed of sites Ge1, O1, O2 and O3 is closer to a regular tetrahedron than a trigonal pyramid.

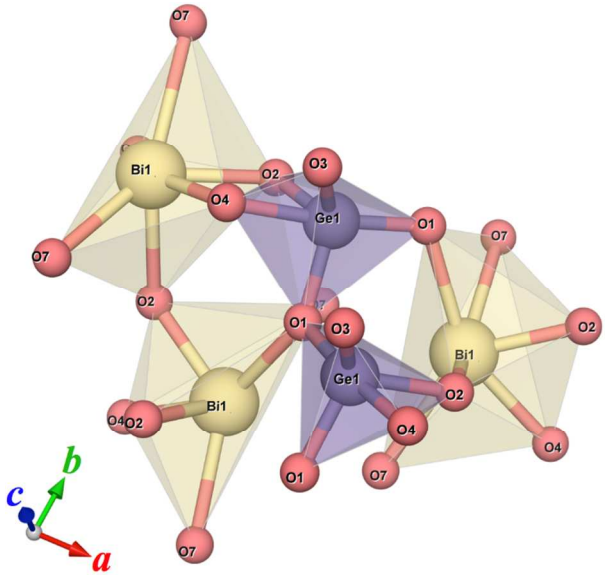

Fig. 6. A local arrangement of GeO4(OH) tbp and BO6 polyhedra.

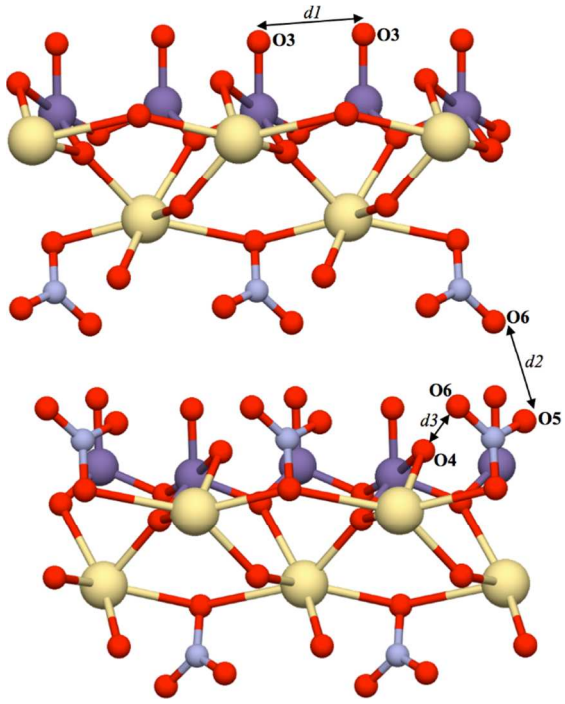

Fig. 7.Presumed local hydrogen bond obtained from the crystal structure model.

The local environments of site Ge1 was determined to have one terminal hydroxyl group each, i.e., Ge–OH. Site O3

bonding to site Ge1 was attributed to OH groups. This coincides with the presence of an absorption peak derived from the Ge–OH in the FT-IR spectrum as shown in Fig. 4. The location of hydrogen bond was presumed by obtained structural model as shown in Fig. 7, although a proton position cannot be pinpointed except for site O3. The interatomic distance of O3–O3 between adjacent GeO_5 tbps ($d1$), of O5–O6 between adjacent NO_3 ions ($d2$), and of O4–O6 between adjacent NO_3 ion and BiO_6 ($d3$), was estimated as 0.2930(15) nm, 0.3013(14) nm and 0.2863(13) nm, respectively. This finding is agreement with the result of ^{1}H NMR experiment. However, the existence of the hydrogen bond of O5–O6 is minor because resonance peaks at 0.9 ppm and 1.3 ppm are much weak. Then, we assumed that site O4 could be attributed to hydroxyl group. Since the atomic displacement parameters, U, of site N1, O5 and O6 attributed to NO_3^- ion converged to very large value in comparison with that of other sites, NO_3^- ion would be vibrating locally (Table 2).

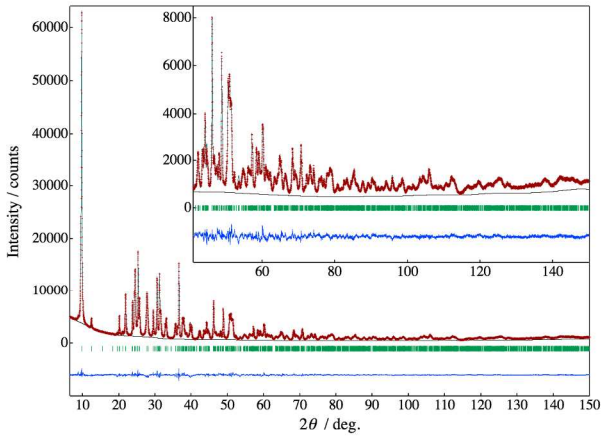

Fig. 8.Observed, calculated, and difference patterns for BGNHO after the Rietveld refinement plotted against 2θ. Green bars and blue curves are the peak position and difference between the observed and calculated intensity values, respectively.

In this way, we proposed the most probable crystal structure of BGNHO composed of one Ge site, one Bi site, one N site and seven O sites. In the early stages of the refinement, we imposed restraints upon all Ge–O bond lengths (i.e., l(Ge–O) = 0.175 ± 0.025 nm) and all O–Ge–O bond angles (i.e., ϕ(O–Ge–O) = 109.5 ± 10.0° and 180 ± 5.0°). In consideration of tbp structure, the restrain of bond angle was set in the wide range. Degrees of restraints were gradually decreased with progression in structure refinements. Although the crystal shape is platy, the influence of preferred orientation (PO) effect along several hkl vectors could not be identified by the refinement. Then, no PO correction was adopted in the final refinement. Additionally, the influence of coarse particles was not confirmed from the omega scan of several strong reflections. The isotropic atomic displacement parameters, U, for the O and N sites were constrained to be equal: U(N1) = U(On: n = 1–7). The U value was fixed at 4.4 (nm^2) for convenience, because the U parameter was estimated to be an inadequately large value (10.1, i.e. B = 8 Å^2) by refinement. This is derived from insufficient data quality (e.g. use of Cu Kα_{12}; heavy atom content; reflections strongly overlapping). The highly disordered distribution of nitrate ion will lead a large U value. Therefore, the constraint of U parameter in light element was applied to obtain more realistic values. The final structural model was visualized using the program VESTA3.[50]

We next evaluated the validity of the O site positions around Bi or Ge site in the obtained model by means of the bond-valence sum (BVS) rule.[51] The bond-valence parameters of Ge^{4+} and Bi^{3+} are given as 1.748 and 2.094, respectively.[52] The effective coordination numbers of Ge and Bi sites were also calculated from refined atomic distances. The BVS values of sites Bi1 and Ge1 were 3.1 and 5.1, respectively. The effective coordination numbers of sites Bi1 and Ge1 were 4.4 and 4.7, respectively. The obtained BVS value of Bi1 coincides with an ideal value. Although, interpretation of the coordination number for the Bi atom was difficult due to the inert-pair effect as mentioned above, the coordination number at Bi1 is six. On the other hand, the BVS of Ge1 is much larger than the desired value, however this value is decreased to 4.3 when site O4 is excluded from the calculation. This indicates that actual coordination number at Ge1 would be close to four and GeO_5 tbp structure would be formed accidentally because site O4 approaches site Ge1. From these reasons, it was considered that site O4 is hydroxyl group which accompanies a Bi atom. Then, the chemical formula of the tbp unit is estimated as $GeO_3(OH)_2$.

Table 1. PXRD Experimental Conditions and Crystallographic Data.

Compound name	BGNHO
Chemical formula	$BiGeO_2(OH)_2{\cdot}(NO_3)$
F_W 408.63 (Z = 8)	
Space group	*Pbca* (No. 61, set 1)
a (nm)	1.145510(10)
b (nm)	0.495346(5)
c (nm)	1.81676(2)
V (nm^3)	1. 03087(2)
Wavelength, λ (nm)	0.154062 (Cu Kα_{12})
2θ range (°)	6.5–150
Step size (2θ) (°)	0.01
Profile range in FWHM	10
No. observations	14351
No. reflections	2533
No. refined structural parameters	36
No. background coefficients	11
R_{wp}	0.0465
R_p	0.0346
R_F	0.0081
R_{Bragg}	0.0133
R_e	0.0235
χ_2	3.93

No other guest-atom/molecule sites were detected in an interlayer space by difference Fourier map. The population of NO_3^- ion was estimated as 8 molecules per unit-cell. A structural defect or a positional disorder was hardly detected by Rietveld analysis. After the final structure refinement, the *R* factors were sufficiently low at R_{wp} = 4.65%, R_{Bragg} = 1.33%, *and* R_F = 0.81%. Experimental conditions and crystallographic information for BGNHO are summarized in Table 1. The refined structural and geometric parameters are listed in Tables 2 and 3, respectively. Observed, calculated, and difference patterns for BGNHO after the Rietveld refinements are plotted against 2θ in Fig. 8.

Table 2. Refined Atomic Coordinates and Isotropic Atomic Displacement Parameter (U) for BGNHO.

Site	*M*	*g*	*x*	*y*	*z*	*U* (nm^2)
Bi1	8c	1.0	0.39764(5)	0.37286(13)	0.18784(3)	0.934(7)
Ge1	8c	1.0	0.31628(13)	0.57188(4)	0.82657(11)	1.03(5)
O1	8c	1.0	0.2002(7)	0.1023(28)	0.2890(5)	4.43*
O2	8c	1.0	0.4458(8)	0.4207(26)	0.7823(5)	= *U*(O1)
O3	8c	1.0	0.3184(8)	0.5676(21)	0.9208(5)	= *U*(O1)
O4	8c	1.0	0.5576(8)	0.2688(21)	0.1243(5)	= *U*(O1)
N1	8c	1.0	0.8956(16)	0.5859(26)	0.9096(7)	= *U*(O1)
O5	8c	1.0	0.9707(8)	0.7352(22)	–0.0758(6)	= *U*(O1)
O6	8c	1.0	0.6404(8)	–0.0779(21)	0.9566(5)	= *U*(O1)
O7	8c	1.0	0.1489(8)	0.400(24)	0.1524(5)	= *U*(O1)

Table 3. Selected Geometric Parameters for BGNHO.

	l (nm)		*φ* (°)
Ge1–O1	0.1726(11)	O3– Ge1–O1	113.6(5)
Ge1–O1	0.1762(14)	O3– Ge1–O1	113.1(5)
Ge1–O2	0.1847(11)	O3– Ge1–O2	114.8(4)
Ge1–O3	0.1712(10)	O3– Ge1–O4	61.2(4)
Ge1–O4	0.1873(10)	O1– Ge1–O1	102.8(4)
		O1– Ge1–O2	104.1(5)
Average	0.1784	O1– Ge1–O4	173.5(5)
		O1– Ge1–O2	83.2(4)
Bi1–O7	0.2485(12)	O1– Ge1–O4	76.0(3)
Bi1–O2	0.2316(11)	O2– Ge1–O4	112.8(5)
Bi1–O2	0.2134(11)		
Bi1–O7	0.2744(11)		
Bi1–O4	0.2226(9)	O5– N1–O7	118(2)
Bi1–O1	0.2435(11)	O5– N1–O6	120(2)
		O7– N1–O6	121(2)
Average	0.2396		
		Average	120
N1–O5	0.116(20)		
N1–O6	0.125(17)		
N1–O7	0.124(17)		
Average	0.122		

In order to verify the validity of the structure model of BGNHO determined by PXRD analysis, we attempt direct observation by HAADF-STEM. Fig. 9(a) shows the thin plate morphology composed of layered structure. The interlayer distance was estimated to be 0.90 nm which is in well agreement with half of the lattice constant of ***c***-axis. Fig. 9(b) shows the atomic resolution image of the sample viewed along [100] direction. In each layer, the atomic columns attributed to Bi or Ge atom are arrayed. The interatomic distances between alternate atomic column along [010] direction were estimated as ca. 0.49 nm, which coincides with the lattice constant of ***b***-axis. In this way, observed images strongly support that BGNHO possess the layered structure as depicted in Fig. 5. It should be noted that structure collapse takes place easily in BGNHO by the electron beam damage.

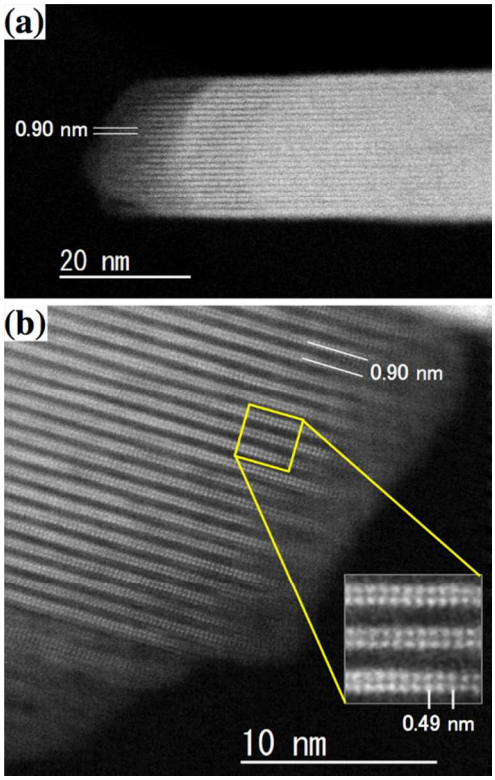

Fig. 9.HAADF-STEM images of BGNHO. (a) shows the thin platy crystalline of BGNHO viewed along [110] direction. (b) shows the atomic resolution image of layered structure composed of Bi and Ge atoms viewed along [100] direction. The inset indicate the magnified image of the layered framework.

The structural formula of BGNHO was estimated as $BiGeO_2(OH)_2(NO_3)$ (Z = 8). If dehydration-condensation between adjacent OH groups and release of NO_3^- ions were to take place in BGNHO, the structural formula would be altered to $Bi_2Ge_2O_5$. In this case, the total weight loss could be estimated as ca. 18.0 wt%, which was in accordance with that observed in TG curve. Actually, by heating BGNHO at 873 K for 3 h in air, BGNHO was changed into the highly crystalline $Bi_4Ge_3O_{12}$[53] and α-quartz-type GeO_2[54] as shown in Fig. 10. Referring to the phase diagram of a quasi-binary Bi_2O_3–GeO_2 system,[55,56] the composition of Bi:Ge = 1:1 at which

corresponds to 66.7 mol% GeO_2 exist in a two-phase state, with coexisting regions of $Bi_4Ge_3O_{12}$ and $Bi_2Ge_3O_9$ phases when the equilibrium state is achieved, or as regions of coexisting $Bi_4Ge_3O_{12}$ and GeO_2 phases when the sample is in its metastable state. Moreover, the sample with composition near $Bi_4Ge_3O_{12}$ is reported to be maintained in its metastable state;[56] these facts suggest that GeO_2 would be formed as the metastable phase. While the reason for this contradiction has not been clarified at the present time, it is likely that the metastable GeO_2 phase would be formed at temperatures higher than 753 K.

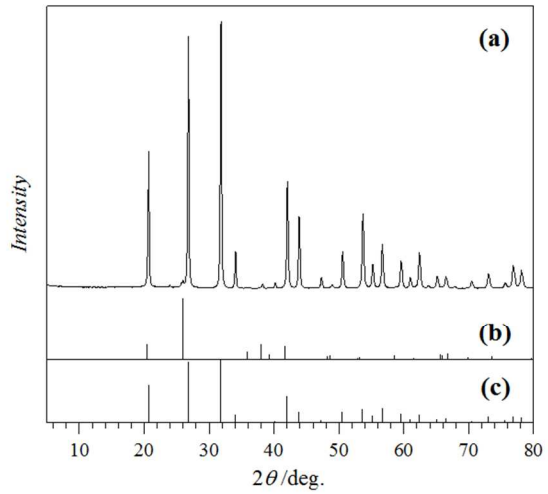

Fig. 10. (a) XRD pattern of the powder sample prepared by heating BGNHO at 873 K for 3 h in air. The reported patterns of (b) α-quartz-type GeO_2[53] and (c) $Bi_4Ge_3O_{12}$[54] are also plotted for comparison.

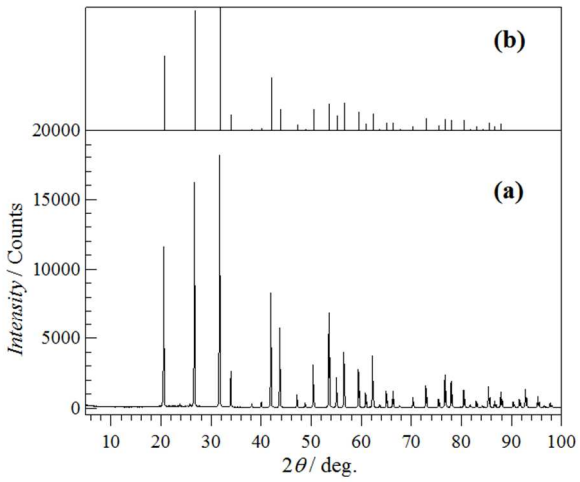

Fig. 11. XRD of the sample prepared by dispersion of BGNHO in ammonia solution for 30 min at room temperature (a). The XRD pattern of the $Bi_4Ge_3O_{12}$ is plotted for comparison.

One applicable property of this new compound becomes the precursor for room temperature synthesis of $Bi_4Ge_3O_{12}$ compound which is a famous X-ray and γ-ray scintillator material. We have already confirmed that the $Bi_4Ge_3O_{12}$ powder can be synthesized by dispersion of the new compound in ammonia solution for about 30 min at room temperature as shown in Fig. 11, even though heating temperature at higher than 1073 K is necessary for the $Bi_4Ge_3O_{12}$ synthesis by the sol-gel method.[25]

Conclusion

We have discovered the formation of a new crystalline phase from an aqueous solution containing Bi_2O_3, GeO_2, nitric acid, ammonia, and distilled water at room temperature and atmospheric pressure. Suitable and reproducible procedures were found to exist for preparation of the homogeneous aqueous solution. The new crystalline phase was found to be composed of a hydrated bismuth germanium nitrate structure. The molecular formula of the new phase can be represented by $BiGeO_2(OH)_2(NO_3)$. The new phase was established as having a layered structure composed of GeO_5 trigonal bipyramid and BiO_6 polyhedra, and was shown to accommodate NO_3^- ions in the interlayer as a guest molecule. Although the actual location of protons was ambiguous, they were well presumed by FT-IR and MAS-NMR spectroscopy. This synthesis method is sustainable route because of no heating process. Further research of the $BiGeO_2(OH)_2{\cdot}(NO_3)$ phase is now in advance as precursor for low-temperature synthesis on $Bi_4Ge_3O_{12}$ compound.

Notes and references

[a] Materials Processing Unit, National Institute for Materials Science, 1-2-1, Sengen, Tsukuba, Ibaraki 305-0047, Japan. Fax: +81-29-859-2501; Tel: +81-29-860-4562; E-mail: KOBAYASHI.kiyoshi@nims.go.jp
[b] Research Center for Compact Chemical System, National Institute of Advanced Industrial and Science and Technology, Nigatake, Sendai, Miyagi 983-8551, Japan. Fax: +81-22-237-5217; Tel: +81-22-237-3016; E-mail: Takuji-ikeda@aist.go.jp

† Footnotes should appear here. These might include comments relevant to but not central to the matter under discussion, limited experimental and spectral data, and crystallographic data.

Electronic Supplementary Information (ESI) available: [crystal structure data in BGNHO.cif]. See DOI: 10.1039/b000000x/

1. M. Ishii and M. Kobayashi, *Prog. Cryst. Growth and Charact. Mater.*, 1991, **23**, 245-311.
2. S. R. Cherry, *Nucl. Instr. Methods in Phys. Res. Sect. A*, 1994, **348**, 577-582.
3. G. Blasse, *Chem. Mater*, 1994, **6**, 1465-1475.
4. M. A. Verdier, P. C. F. Di Stefano, P. Nadeau, C. Behan, M. Clavel and C. Dujardin, *Physical Review B*, 2011, **84**.
5. I. Valais, C. Michail, S. David, C. D. Nomicos, G. S. Panayiotakis and I. Kandarakis, *Physica Medica*, 2008, **24**, 122-125.
6. X. Y. Sun, D. G. Jiang, W. F. Wang, C. Y. Cao, Y. N. Li, G. T. Zhen, H. Wang, X. X. Yang, H. H. Chen, Z. J. Zhang and J. T. Zhao, *Nucl. Instr. Methods in Phys. Res. Sect. A*, 2013, **716**, 90-95.
7. P. M. Lambert, *Inorg. Chem*, 1998, **37**, 1352-1357.
8. P. M. Lambert, *Mater. Res. Bull.*, 2000, **35**, 383-391.
9. L. León-Reina, M. C. Martin-Sedeño, E. R. Losilla, A. Cabeza, M. Martinez-Lara, S. Bruque, F. M. B. Marques, D. V. Sheptyakov and M. A. G. Aranda, *Chem. Mater*, 2003, **15**, 2099-2108.
10. S. Nakayama, Y. Higuchi, Y. Kondo and M. Sakamoto, *Solid State Ionics*, 2004, **170**, 219-223.
11. A. Orera and P. R. Slater, *Chem. Mater*, 2010, **22**, 675-690.
12. S. F. Wang, Y. F. Hsu, W. J. Lin and K. Kobayashi, *Solid State Ionics*, 2013, **247**, 48-55.

13. H. Mizoguchi, T. Kamiya, S. Matsuishi and H. Hosono, *Nature Comm.*, 2011, **2**.
14. A. Jha, B. Richards, G. Jose, T. Teddy-Fernandez, P. Joshi, X. Jiang and J. Lousteau, *Prog. Mater. Sci.*, 2012, **57**, 1426-1491.
15. R. Stepien, D. Pysz, I. Kujawa and R. Buczynski, *Opt. Mater.*, 2013, **35**, 1587-1594.
16. O. D. Lyakh, I. A. Sheka and A. I. Perfil'ev, *Russ. J. Inorg. Chem.*, 1965, **10**, 993-996.
17. V. Vekhov, V., B. S. Vitukhnovskaya and R. F. Doronkina, *Russ. J. Inorg. Chem.*, 1966, **11**, 132-135.
18. S. P. Mukherjee, A. S. Glass and M. J. D. Low, *J. Am. Ceram. Soc.*, 1990, **73**, 242-244.
19. C. B. Jing, J. X. Hou and Y. H. Zhang, *J. Cryst. Growth*, 2008, **310**, 391-396.
20. D. D. Tuschel and P. M. Lambert, *Chem. Mater*, 1997, **9**, 2852-2860.
21. E. Frolova, *Mater. Sci. & Eng. C*, 2003, **23**, 1093-1097.
22. E. V. Frolova and M. I. Ivanovskaya, *Solid State Ionics*, 2004, **173**, 125-130.
23. S. D. V. Serezhkina, E. A. Tyavlovskaya, G. P. Shevchenko and S. K. Rakhmanov, *J. Non-Cryst. Solids*, 2005, **351**, 35-40.
24. F. A. A. de Jesus, M. R. B. Andreeta, A. C. Hernandes and Z. S. Macedo, *Opt. Mater.*, 2010, **32**, 1286-1290.
25. F. A. A. de Jesus, R. S. da Silva and Z. S. Macedo, *J. Thermal Anal. Calor*, 2010, **100**, 537-541.
26. A. Orera and P. R. Slater, *Proc. Ntnl Acad; Sci; India Sect. A*, 2012, **82**, 43-48.
27. K. Kobayashi, *Japanese Unexamined Patent Application Publication No. 2013-060333*, 2014.
28. S. Kitajima, K. Kobayashi, T. Higuchi and Y. Sakka, in *Innovative Processing and Manufacturing of Advanced Ceramics and Composites II*, John Wiley & Sons, Inc., 2014, pp. 103-108.
29. N. Henry, M. Evain, P. Deniard, S. Jobic, F. Abraham and O. Mentre, *Z. Naturforsch. Sect. B*, 2005, **60**, 322-327.
30. N. Henry, O. Mentre, F. Abraham, E. J. MacLean and P. Roussel, *J. Solid State Chem.*, 2006, **179**, 3087-3094.
31. F. N. Shi, L. Cunha-Silva, F. A. A. Paz, M. J. Hardie, J. Klinowski, J. Rocha and T. Trindade, *Inorg. Chem Comm.,* 2008, **11**, 283-287.
32. S. I. Troyanov, A. V. Kostrikin, F. M. Spiridonov, B. E. Zaitsev, S. V. Tarasova and O. V. Kosenkova, *Crystallogr. Rep.*, 2006, **51**, 414-418.
33. H. S. Yang and B. J. Finlayson-Pitts, *J. Phys. Chem. A*, 2001, **105**, 1890-1896.
34. S. G. Moussa, A. C. Stern, J. D. Raff, C. W. Dilbeck, D. J. Tobias and B. J. Finlayson-Pitts, *Phys. Chem. Chem. Phys.,* 2013, **15**, 448-458.
35. K. Nakamoto, in *Infrared and Raman Spectra of Inorganic and Coordination Compounds*, John Wiley & Sons, Inc., 2008, pp. 182-183.
36. J. Mason, L. F. Larkworthy and E. A. Moore, *Chemical Reviews*, 2002, **102**, 913-934.
37. R. Marek and A. Lycka, *Curr. Organ. Chem.*, 2002, **6**, 35-66.
38. S. Hayashi and K. Hayamizu, *Bull. Chem. Soc. Jp*, 1991, **64**, 688-690.
39. H. Eckert, J. P. Yesinowski, L. A. Silver and E. M. Stolper, *J. Phys. Chem.*, 1988, **92**, 2055-2064.
40. A. A. Bolzan, C. Fong, B. J. Kennedy and C. J. Howard, *Acta Crystallogr. Sect. B*, 1997, **53**, 373-380.
41. A. Altomare, N. Corriero, C. Cuocci, A. Moliterni and R. Rizzi, *J. Appl. Crystallogr.*, 2013, **46**, 779-787.
42. A. Lebail, H. Duroy and J. L. Fourquet, *Mater. Res. Bull.*, 1988, **23**, 447-452.
43. G. Oszlanyi and A. Suto, *Acta Crystallogr. Sec. A*, 2004, **60**, 134-141.
44. L. Palatinus and G. Chapuis, *J. Appl. Crystallogr.*, 2007, **40**, 786-790.
45. H. L. Li, M. Eddaoudi and O. M. Yaghi, *Angew. Chem.-Interntnl. Ed.*, 1999, **38**, 653-655.
46. Q. Liu, Y. Zhou, W. G. Tu, S. C. Yan and Z. G. Zou, *Inorg. Chem*, 2014, **53**, 359-364.
47. F. A. Cotton and G. Wilkinson, *Adv. Inorg. Chem*, 1988, **5th ed.**, 22-27, 208-209.
48. V. Favre-Nicolin and R. Cerny, *J. Appl. Crystallogr.*, 2002, **35**, 734-743.
49. F. Izumi and K. Momma, *Solid State Phenom.*, 2007, **130**, 15-20.
50. K. Momma and F. Izumi, *J. Appl. Crystallogr.*, 2011, **44**, 1272-1276.
51. I. D. Brown and D. Altermatt, *Acta Crystallogr. Sect. B,* 1985, **41**, 244-247.
52. International Union of Crystallography. Bond Valence Parameters. http://www.iucr.org/resources/data/datasets/bond-valence-parameters (2013 version).
53. S. F. Radaev, L. A. Muradyan, Y. F. Kargin, V. A. Sarin, V. N. Kanepit and V. I. Simonov, *Kristallogr*, 1990, **35**, 361-364.
54. J. Haines, O. Cambon, E. Philippot, L. Chapon and S. Hull, *J. Solid State Chem.*, 2002, **166**, 434-441.
55. P. Tissot and H. Lartigue, *Thermochim. Acta*, 1988, **127**, 377-383.
56. G. Corsmit, M. A. Vandriel, R. J. Elsenaar, W. Vandeguchte, A. M. Hoogenboom and J. C. Sens, *J. Cryst. Growth*, 1986, **75**, 551-560.

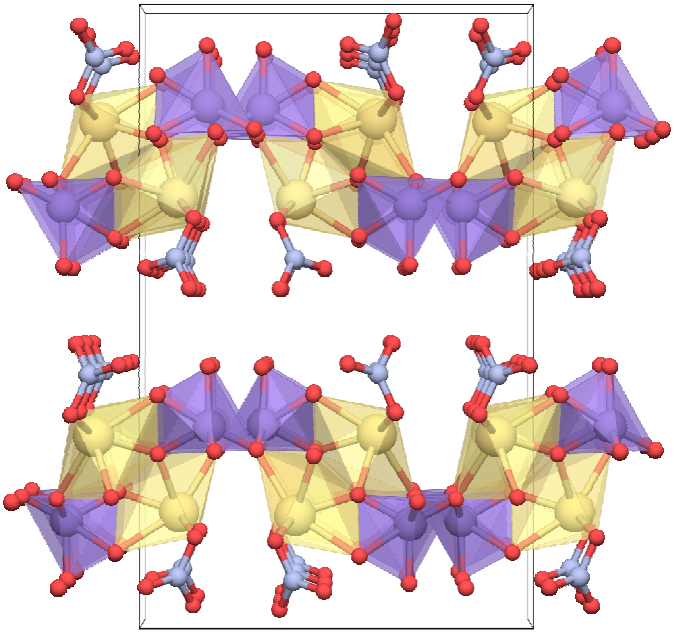

A new crystalline phase, $BiGeO_2(OH)_2(NO_3)$ has been synthesized from a homogeneous aqueous solution. This new phase is found to possess a layered structure consisting of BiO_6 polyhedra, GeO_5 trigonal bipyramids and nitrate ions.